

# Multianalyte Antibiotic Detection on an Electrochemical Microfluidic Platform

**Journal Article****Author(s):**

Kling, André; Chatelle, Claire; Ambrecht, Lucas; Qelibari, Edvina; Kieninger, Jochen; Dincer, Can; Weber, Wilfried; Urban, Gerald

**Publication date:**

2016-10-18

**Permanent link:**

<https://doi.org/10.3929/ethz-b-000121963>

**Rights / license:**

[In Copyright - Non-Commercial Use Permitted](#)

**Originally published in:**

Analytical Chemistry 88(20), <https://doi.org/10.1021/acs.analchem.6b02294>

# Multianalyte Antibiotic Detection on an Electrochemical Microfluidic Platform

André Kling,<sup>†,||,⊥</sup> Claire Chatelle,<sup>‡,⊥</sup> Lucas Armbricht,<sup>†,||</sup> Edvina Qelibari,<sup>†</sup> Jochen Kieninger,<sup>†</sup> Can Dincer,<sup>\*,†,§</sup> Wilfried Weber,<sup>‡</sup> and Gerald Urban<sup>†,§</sup>

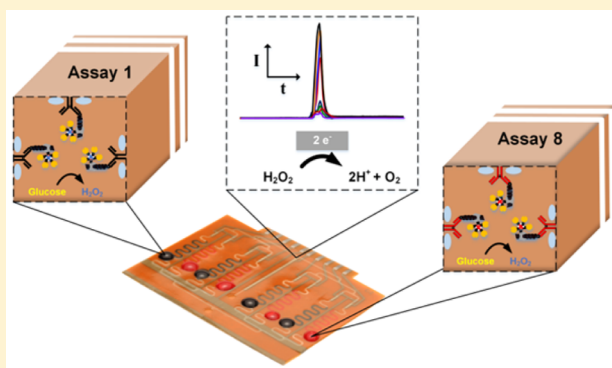
<sup>†</sup>University of Freiburg, Department of Microsystems Engineering, Georges-Koehler-Allee 103, DE-79110 Freiburg, Germany

<sup>‡</sup>University of Freiburg, Faculty of Biology and Centre for Biological Signalling Studies, Schänzlestraße 18, DE-79104 Freiburg, Germany

<sup>§</sup>University of Freiburg, Freiburg Materials Research Center, Stefan-Meier-Straße 21, DE-79104 Freiburg, Germany

## S Supporting Information

**ABSTRACT:** The excessive use of antibiotics in human and veterinary medicine causes the emergence of multidrug resistant bacteria. In this context, the surveillance of many different antibiotics provokes a worldwide challenge. Hence, fast and versatile multianalyte single-use biosensors are of increasing interest for many fields such as medical analysis or environmental and food control. Here we present a microfluidic platform enabling the electrochemical readout of up to eight enzyme-linked assays (ELAs), simultaneously. To demonstrate the applicability of this platform for the surveillance and monitoring of antibiotics, we used highly sensitive biomolecular sensor systems for the simultaneous detection of two commonly employed antibiotic classes tetracycline and streptogramin. Thus, microfluidic channel networks are designed, comprising distinct numbers of immobilization sections with a very low volume of 680 nL each. These passively metered sections can be actuated separately for an individual assay procedure. The limits of detection (LOD) are determined, with high precision, to 6.33 and 9.22 ng mL<sup>-1</sup> for tetracycline and pristinamycin, respectively. The employed channel material, dry film photoresist (DFR), allows an easy storage of preimmobilized assays with a shelf life of at least 3 months. Multianalyte measurements in a complex medium are demonstrated by the simultaneous detection of both antibiotics in spiked human plasma within a sample-to-result time of less than 15 min.



The request for fast, precise, and comprehensive bio-analytical information, obtained from enzyme-linked assays (ELAs), concerns the fields of medicine, environmental, and food control.<sup>1</sup> In this regard, point-of-care (POC) monitoring is steadily promoted to reduce sample volumes and laboratory turnaround times.<sup>2–4</sup> Especially the detection of multiple analytes obtained from a very low sample volume provokes the development of multiplexed sensor platforms.<sup>5</sup> Although different miniaturized diagnostic systems have been developed in recent years,<sup>6</sup> still a lot of challenges remain, including technical (e.g., simplicity and sensitivity) and nontechnical (e.g., acceptance in clinical practice) barriers.<sup>7,8</sup> By overcoming these challenges, the development of fast, simple, and cheap on-site multianalyte sensors will have a big impact to a very wide range of applications.

An urgent example for the application of multiplexed sensors is given by the global combat against antimicrobial resistance. Because of the excessive and inappropriate use of antibiotics, multidrug-resistant bacteria have spread all over the world provoking an increasing number of life-threatening infections difficult to treat with currently available medicines.<sup>9</sup> To solve

the problem at the root, the World Health Organization (WHO) stated an action plan including the regulation and survey of the overuse of antibiotics in human or veterinary medicine and as growth promoters in stock farmings.<sup>10</sup>

For the measurement of antibiotics, traditional microbiological tests based on bacterial growth inhibition can be used. Despite their simplicity and low costs, they are time-consuming and must be performed in the laboratory.<sup>11</sup> Alternative methods including liquid chromatography (LC) coupled to mass spectrometry (LC–MS) or UV (LC–UV) detection and capillary electrophoresis (CE) based methods require extensive sample preparation, are expensive, and can only be performed by trained personnel.<sup>11</sup> The detection of specific antibiotics can in some cases also be done with common antibodies.<sup>12</sup> They provide a high specificity and sensitivity but do not provide enough stability and suffer from

Received: June 13, 2016

Accepted: July 19, 2016

Published: July 19, 2016

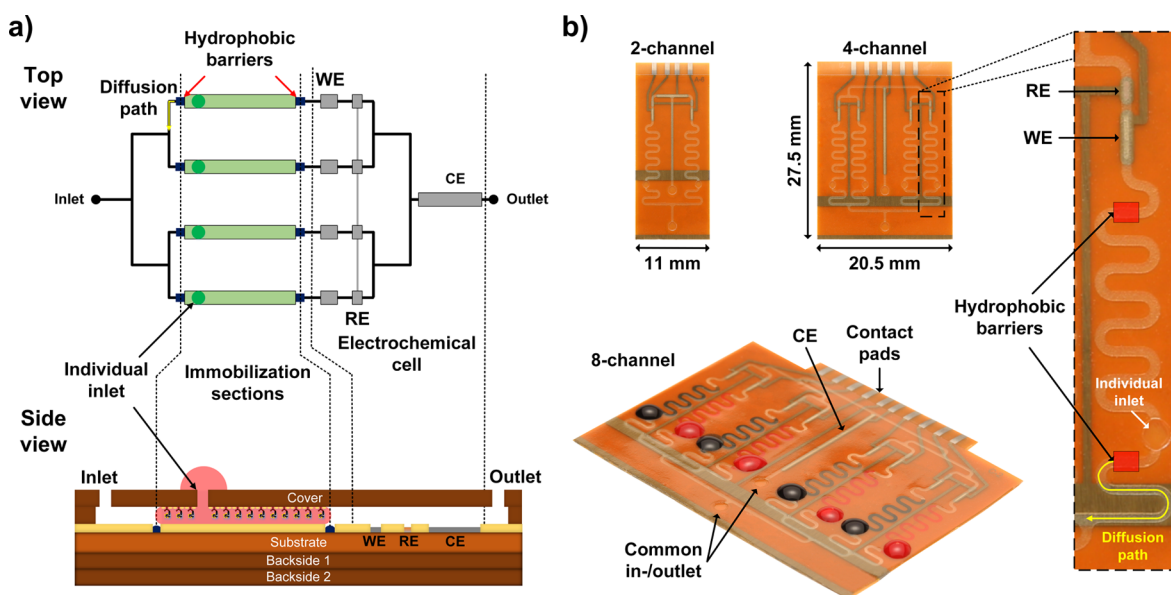


**Figure 1.** (a) Schematic top and side view of the microfluidic multiplexed platform. Different immobilization sections (green) in combination with a single electrochemical cell including multiple working electrodes (WEs), counter (CE) and reference electrodes (RE) are arranged in a microfluidic network. Assay reagents (red) are loaded via the individual inlets by capillary force. (b) Photographs of the microfluidic biosensors comprising either two, four, or eight immobilization sections. Each immobilization section (of the 8 channel chip) is loaded with another assay reagent (red or black), passively metered by the hydrophobic barriers. A diffusion path is introduced to prevent any cross-talk between neighboring channels during the simultaneous readout.

batch-to-batch variations.<sup>13</sup> To screen for an unknown antibiotic, a single measurement platform for the simultaneous on-site monitoring of commonly used antibiotic classes (e.g., tetracyclines and streptogramins) would offer great advantages.<sup>14</sup>

In such cases, the use of naturally occurring sensor systems seems to be a promising alternative to antibodies. Bacteria resistant to tetracyclines or streptogramins, for example, can sense environmental antibiotics and induce the expression of efflux pumps to actively pull antibiotics out of the cell and survive.<sup>15</sup> In those bacteria, the sensing system relies on an operator DNA and a repressor protein pair in which interaction is modulated by antibiotics. In the absence of antibiotics, the repressor protein is tightly bound to the operator DNA, preventing expression of the pump. If a specific class of antibiotics is present, the repressor detaches from the operator, inducing expression of the pump and survival of the bacterium. Those operator/repressor sensing systems are evolutionarily optimized by bacteria to detect a specific class of antibiotics at biologically relevant concentrations. Additionally, they can be relatively easily and cheaply synthesized and transposed to a cell free environment for convenient handling and readout which make them outstanding tools for the development of multiantibiotics assays. On the basis of this mechanism, the development and investigation of class-specific ELAs sensitive to streptogramins and tetracyclines were previously presented.<sup>16</sup>

A cheap, fast, highly sensitive, and easy-to-handle sensor for such assays, would meet major demands for the detection of various analytes from a variety of sample formats (e.g., food, blood, urine, and saliva). Regarding the platforms for a simultaneous on-site readout of ELAs, they can be divided into four major categories. First, multianalyte detection, driven by the necessity for high-throughput genomic and proteomic screening methods,<sup>17</sup> can be achieved by highly dense array-based systems. High numbers of reagent spots in the range of

nano- to picoliter are printed on a solid surface and read out with optical or electrochemical methods.<sup>18–20</sup> Although efforts have been made to miniaturize those systems, they remain difficult to use for on-site measurements. The use of microbeads is also a frequently proposed method for the high-throughput readout of multiple assays. Their flexibility in size and surface coating offer good advantages for laboratory diagnostics, but these systems stay too complicated for the application in resource limited settings.<sup>21–26</sup> Among the systems proposed for on-site measurements, test-strips and lateral flow assays, fast, cheap, and easy-to-handle, are often the method of choice, but they generally only allow a qualitative detection of a single or limited number of analytes.<sup>27,28</sup> For multianalyte POC detection, the application of microfluidic systems offers a good possibility to achieve lab-on-a-chip multiplexing with low complexity and miniaturization.<sup>29,30</sup> Their high surface-to-volume ratio facilitates faster and more sensitive reactions as well as a very low reagent consumption.<sup>31</sup> For the design of microfluidic devices, different aspects must be considered, including the employed channel material, assay immobilization, and readout technique.<sup>32</sup> In this context, electrochemical sensors are favorable due to their great potential for miniaturization along with a low power consumption and high sensitivity.<sup>33–35</sup>

In summary, there is a high demand for multiplexed detection systems, especially with regard to POC applications.<sup>36,37</sup> In this context, we present the development of a disposable, microfluidic biosensor, to detect up to eight different analytes. Simultaneous electrochemical readout of different ELAs is achieved without the use of any external active valving system. The chip fabrication is adapted and optimized from a previously presented dry film photoresist (DFR) based single-channel sensor.<sup>38</sup> Finally, the multiplexing applicability of this platform is demonstrated by the simultaneous measurement of two antibiotics in human plasma using the advantages of the described DNA–protein interaction sensing mechanism.

## EXPERIMENTAL SECTION

**Chip Design.** The employed chip design relies on a strict separation between the assay immobilization region and the electrochemical readout cell. Thus, the assay is immobilized on the surface of a well-defined section of a microchannel. A similar approach, employing DFR as a channel material, was previously presented by our group.<sup>39</sup> Thereby, the chip is composed of a single microchannel with an in- and outlet, a certain region for the assay immobilization, and an electrochemical cell for the enzyme-mediated readout. To transfer the same principle to a multiplexed detection, on a single chip, a microfluidic channel network, as illustrated in Figure 1a, is implemented. For the simultaneous readout, the different assays are immobilized in distinct sections of this network and simultaneously read out again with a single electrochemical cell in the downstream channel. Hence, the incorporation of immobilization sections within a microfluidic network and their simultaneous actuation via a common in- and outlet enables the quantification of multiple assays with the same effort as for a single analyte. By connecting several of these immobilization sections in parallel, the network can be easily described by electronic circuitry.<sup>40</sup> Here, it must be assured that the fluidic resistances for each channel pathway, from in- to outlet, are the same. This results in an equal volume flow through each path, when a pressure difference is applied from the common in- to the outlet.

In each channel branch of the fluidic network, depicted in Figure 1b, an immobilization section with a volume of 680 nL and a surface-to-volume ratio of  $155 \text{ cm}^{-1}$  is incorporated. Their independent actuation is realized by individual channel openings. This enables a defined capillary filling with assay reagents by pipetting small drops (approximately  $1 \mu\text{L}$ ) on the relevant inlet. The capillary filling is passively metered by two hydrophobic barriers on each end of these sections. Removal of the assay reagents is realized by the application of vacuum to the common inlet and temporary sealing of the individual inlets with sticky tape. This ensures that no biomolecules are flushed over the electrodes of the electrochemical cell while wash buffer is introduced from the common outlet. Such an approach enables a separate and independent immobilization of different assays in each channel branch. For the amperometric signal detection, the microchannel network contains a single electrochemical cell with a three-electrode setup. Thus, multiple Pt working electrodes (WEs,  $0.23 \text{ mm}^2$ ), arranged in each channel branch, share a common on-chip Ag/AgCl pseudo reference (RE,  $0.09 \text{ mm}^2$ ) and Pt counter electrode (CE,  $0.8 \text{ mm}^2$ ). It should be noted that the reference electrode is split up and brought nearby to each working electrode to avoid an ohmic drop.

For the measurement, the individual inlets are permanently sealed with a 1 mm thick PMMA piece and double sided tape. This enables the connection of the channel network to the substrate solution reservoir via the common in-and outlet. A pressure driven flow from the common in- to the outlet is induced by a syringe pump. A custom-made chip holder is developed for the electrical and fluidic connection to the syringe pump. Simultaneous amperometric measurements are realized with a multiplexer potentiostat.

**Chip Fabrication.** For a low-cost and disposable platform, the fabrication of the fluidic chip mainly relies on polymer materials. In this regard, DFR technology offers the possibility for rapid prototyping without cleanroom equipment and

processing with low-cost foil masks. Furthermore, it is possible to immobilize biomolecules on its surface via covalent and noncovalent methods. The wafer-level fabrication, presented in Figure 2, begins with the preparation of a  $50 \mu\text{m}$  thick

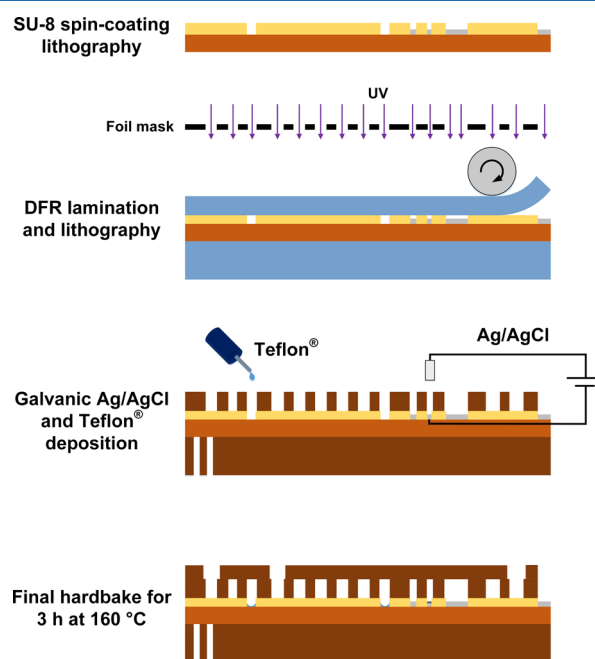


**Figure 2.** Illustration of different fabrication steps of the microfluidic multiplexed biosensor platform. First, Pt is structured on a PI substrate and isolated with SU-8. Next, the microfluidic channels are realized by lamination of different DFR layers. Later, hydrophobic stopping barriers are enhanced with a Teflon layer and the reference electrodes are created by galvanic deposition. Finally, a cover layer is laminated sealing the microfluidic channels.

polyimide (PI) substrate in a 6 in. format. After removing the copper clad of Pyralux AP8525R (DuPont) in a copper etch bath for 1 h, a rough PI substrate is released. The platinum (Pt) electrodes are directly patterned on the PI surface in a lift-off process. Thus, the resist MA-N 1420 (Micro Resist Technology) is spin coated at 3 000 rpm for 30 s. Subsequently, a 200 nm Pt layer is evaporated by physical vapor deposition in the only clean room process. To ensure a proper isolation and definition of the geometric electrode areas on one hand, but also to define small wells for the fluidic barriers, a  $5 \mu\text{m}$  thick layer of SU-8 3005 (MicroChem Corp.) is spin coated with 4 000 rpm for 30 s.<sup>41</sup> After UV exposure and development, the wafer is hardbaked in an oven for 1 h at  $150 \text{ }^\circ\text{C}$ .

For the implementation of the  $500 \mu\text{m}$  wide microfluidic channels, different layers of the  $63.5 \mu\text{m}$  thick DFR Pyralux PC1025 (DuPont) are realized on the wafer-level. The DFR is laminated with a common office laminator MyJoy 12 (GMP Prographics) at room temperature (RT). Each lamination step is followed by a UV exposure for 2 min 30 s with the appropriate foil mask on an exposure unit Hellas (Bungard Elektronik). After repetition of the lamination and exposure steps to the front- and backside, the wafer is developed for 2 min in an ultrasonic bath with 1% sodium carbonate ( $\text{Na}_2\text{CO}_3$ ) solution at  $42 \text{ }^\circ\text{C}$ . Upon realization of the microfluidic channels, the reaction is stopped in a 1% HCl bath for 1 min. The thermal expansion of the photoresist, occurring in the final hardbake step, is compensated by the lamination of DFR



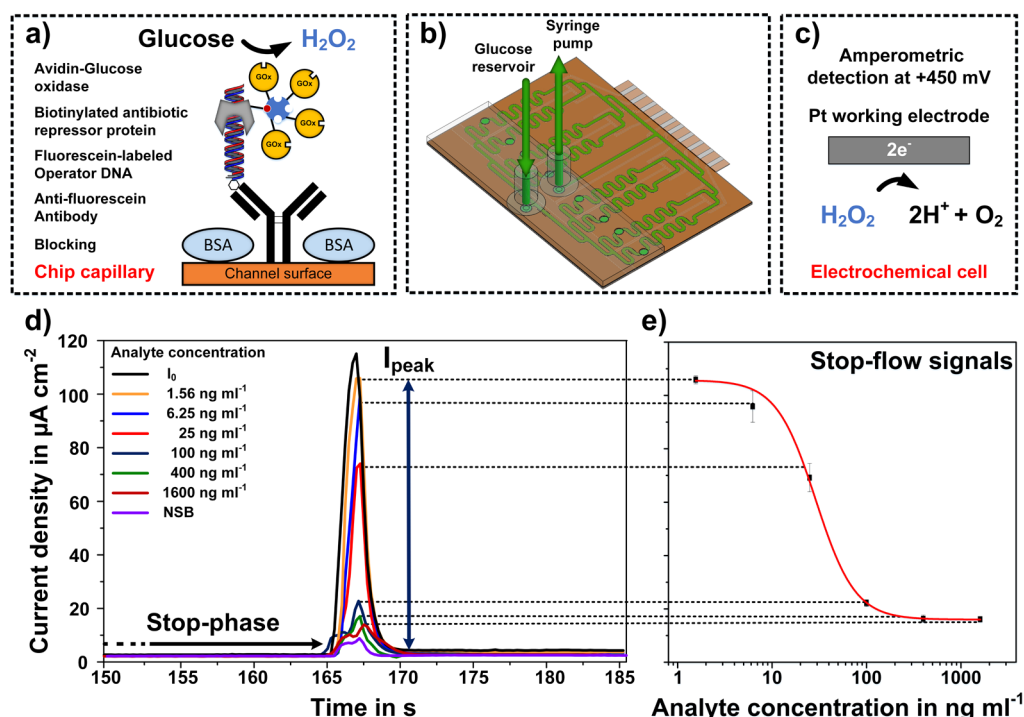


**Figure 3.** Illustration of the measurement principle. (a) The antibiotic assay is immobilized in the different immobilization sections. By supplying the enzyme with glucose, hydrogen peroxide is produced that can be detected again at the respective working electrode. (b) CAD drawing showing the sealing of the individual inlets with a PMMA piece and double-sided tape enabling connection to a glucose reservoir and a syringe pump via vacuum cups. (c) Reaction mechanism of the  $\text{H}_2\text{O}_2$  oxidation at the Pt WE resulting in a concentration dependent current. (d) Stop-flow peaks from a simultaneous amperometric readout of eight immobilization sections with different analyte concentrations. Additionally, the signals for no antibiotic ( $I_0$ ) and the nonspecific binding (NSB) are gauged. (e) Resulting on-chip calibration curve.

layers on the front- and backside of the substrate. An intermediate baking step, for 1 h at 150 °C, improves the chemical resistance for the silver deposition in an alkaline solution. The galvanic deposition of the on-chip Ag/AgCl reference electrodes is also carried out in a wafer-level process. Therefore, all contact pads are passivated by lamination of an UV sensitive adhesive tape 1020R (Ultron Systems Inc.). Subsequently, the deposition of silver onto the Pt reference electrodes is performed in an Arguna S solution (Umicore Galvanotechnik) with an applied current density of  $-16 \text{ mA cm}^{-2}$  for 5 min and a silver wire as the counter electrode. Finally, the resulting silver layer is chlorinated to Ag/AgCl at  $+1.6 \text{ mA cm}^{-2}$  for 10 min with a platinum wire as the counter electrode in a 0.1 M KCl solution. In order to improve the hydrophobicity of the passive fluidic barriers, a small drop of 1% Teflon AF 1600 (DuPont) is dispensed into the physical barriers by a hand dispenser. This forms a thin Teflon coating which stops the capillary filling of the immobilization sections within the channels to a certain extent. Sealing of the microfluidic channels is achieved with a cover layer made of a sheet of Pyralux PC1025 structured on its supporting PET foil with the aforementioned process parameters. Finally, the wafer is diced into individual chips with a common pair of scissors and hardbaked for 3 h at 160 °C. The DFR-based microfluidic multianalyte platforms, with either two, four, or eight immobilization sections are presented in Figure 1c. A detailed illustration of the fabrication procedure is given in the Supporting Information.

**Signal Transduction.** An effective signal transduction of the binding event between biomolecules, suitable to electrochemical detection, is found by the use of glucose oxidase

(GOx) as an enzyme label (see Figure 3a). It catalyzes the reaction from a glucose substrate to hydrogen peroxide ( $\text{H}_2\text{O}_2$ ) that is detected by the electrochemical measurement cell. Depending on the amount of bound analyte of the labeled assay, a characteristic amount of  $\text{H}_2\text{O}_2$  is produced in each immobilization section and measured amperometrically at the respective WE. For the measurement, all working electrodes are polarized to 0.45 V vs the on-chip Ag/AgCl reference electrode.

**Stop-Flow Measurement Technique.** For this platform, signal amplification is achieved by applying a defined stop-flow measurement protocol. When the channel network is constantly supplied with the glucose substrate solution, the bound enzyme GOx generates only a limited amount of  $\text{H}_2\text{O}_2$ . By stopping the flow for a certain time, the enzyme further catalyzes the reaction to  $\text{H}_2\text{O}_2$  within the individual immobilization sections. By restarting the flow, the accumulated clouds are flushed over the respective working electrode. The generated peak signal (see Figure 3d), originating from the  $\text{H}_2\text{O}_2$  oxidation, is hence dependent on the amount of bound enzyme and the stop time. For the signal evaluation, either the peak height or the transferred charge can be investigated.<sup>39</sup>

**Antibiotic Assay.** To evaluate the developed versatile platform, we utilized assays for the detection of two antibiotic classes: tetracyclines and streptogramins in human plasma.<sup>14,16,42</sup> These assays, depicted in Figure 3a, rely on the naturally occurring sensing system which evolved in certain bacteria to resist those antibiotics. The main feature is a repressor protein (TetR or PIP) that binds to a specific operator DNA (*tetO* or *Pir*). In the presence of the class-specific antibiotics, the proteins prove a conformational change and cannot bind to their designated operator DNA. This allows

the implementation of a competitive assay for the quantification of tetracycline and streptogramin antibiotics from clinically relevant samples.

In contrast to a previously described optical detection, the assay is further optimized for the on-chip electrochemical detection in this report.<sup>16</sup> To ensure an easy and universally applicable biomolecule immobilization in the microfluidic channels, anti fluorescein antibodies are used as spacer and capture biomolecules. They are simply adsorbed on the DFR surface and thus prevent any steric hindrance occurring from a blocking step. This enables a fast way to bind fluorescein labeled target biomolecules. The antibiotic sensitive repressor proteins are biotinylated to facilitate a subsequent binding to an avidin-GOx conjugate. After functionalization with anti fluorescein antibodies, the channel surface is blocked with bovine serum albumin (BSA) to exclude any nonspecific binding. The respective operator DNAs, labeled with fluorescein at their 5' end, bind to the adsorbed antibodies. Here, different operator DNAs may be loaded to different immobilization sections of the chip. The biotinylated antibiotic-sensitive repressor proteins and avidin-GOx are added to the sample and introduced in the microfluidic network. Subsequently, unbound proteins are removed in a washing step. The electrochemical signal readout is finally achieved by supplying the network with glucose solution (see Figure 3b–d). The more antibiotic is present, less proteins bind to their operator DNA. This results in a decreased signal, as illustrated in Figure 3e. The employed assay design offers a high flexibility and a total assay time of around 2 h 30 min.

**Repressor Protein Production and Purification.** The repressor proteins TetR and PIP are produced with a C terminal Avi tag for *in vivo* site specific biotinylation by the enzyme BirA, followed by a hexahistidin tag for purification. BL21\* (DE3) is cotransformed with pCVC008 and pBirA for expression of biotinylated TetR (bTetR) protein and BirA enzyme, respectively. BL21\* (DE3) pLysS is transformed with pCVC012 for coexpression of BirA and biotinylated PIP (bPIP). Cells are grown in LB medium supplemented with ampicillin (100  $\mu\text{g mL}^{-1}$ ) and chloramphenicol (34  $\mu\text{g mL}^{-1}$ ) at 37 °C until  $\text{OD}_{600} = 0.6$ . The culture medium is supplemented with 50  $\mu\text{M}$  biotin and protein production is induced with 1 mM  $\beta$ -D-1-thiogalactopyranoside (IPTG) for 4 h at 37 °C for bPIP and overnight at 20 °C for bTetR. Cells are harvested by centrifugation (6 000g, 10 min, RT), resuspended in lysis buffer (35 mL per liter initial culture volume, 50 mM  $\text{NaH}_2\text{PO}_4$ , 300 mM NaCl, 10 mM imidazole pH 8.0), freeze-thawed and lysed by sonication (Bandelin) (60%, pulse 0.5 s every second for 10 min). Subsequently, cells debris are eliminated by centrifugation (30 000g, 30 min, 4 °C). Proteins are purified from the supernatant on a gravity flow  $\text{Ni}^{2+}$ -NTA-agarose Superflow column (Qiagen) following manufacturer instructions.

Protein concentration is determined by the Bradford method (Bio-Rad) using BSA as the standard. Proteins are diluted to 1 mg  $\text{mL}^{-1}$  in elution buffer (50 mM  $\text{NaH}_2\text{PO}_4$ , 300 mM NaCl, 250 mM imidazole pH 8.0) containing 10% sucrose, lyophilized and stored at –80 °C. For each experiment the lyophilized proteins are dissolved in ultrapure  $\text{H}_2\text{O}$  (HPLC grade) (Alfa Aesar).

**Annealing of the Fluorescein Terminated Double Stranded Oligonucleotides (*tetO* and *Pir*).** Oligonucleotides are purchased from Sigma-Aldrich. The double stranded DNA operators *tetO* and *Pir*, required for the binding of the

repressor proteins, are generated by mixing the oligonucleotides oCVC057 (Fluorescein-GCACTCCCTATCAGTGATA GAGAAACG) and oCVC049 (CGTTTCTCTATCACTGATA GGGAGTGC) for *tetO* and oCVC059 (Fluorescein-GCTCG TACACCGTACAAGG) with oCVC050 (CCTTGACGGTG TACGAGC) for *Pir*, in equimolar amounts (50  $\mu\text{M}$  each) in 1× saline-sodium citrate (SSC) buffer (15 mM sodium citrate, 150 mM NaCl, pH 7.0). The solutions are incubated at 95 °C for 5 min followed by slow cooling (2 °C per min) to room temperature.

## RESULTS AND DISCUSSION

All electrochemical measurements are performed in 0.1 M phosphate buffered saline (PBS) pH 7.4 containing 0.1 M NaCl prepared with ultrapure water. For the enzyme-mediated readout, a 40 mM glucose substrate solution is utilized. An EmSTAT3 potentiostat with an 8-channel multiplexer (PalmSens) is employed in constant polarization mode with the delivered software PSTrace 4.6. A constant volume flow is induced by a syringe pump PHD Ultra (Harvard Apparatus).

A short pretreatment of the working electrodes is executed once, with an applied buffer flow of 20  $\mu\text{L min}^{-1}$  per channel. Thus, the WEs are polarized for 5 s to 0.8 and –0.1 V, respectively, for 50 cycles. Additionally, the WEs are oxidized at 0.8 V for 60 s prior to the measurement to enhance the signal stability and sensitivity to  $\text{H}_2\text{O}_2$ .

**Cross-Sensitivity.** A critical point in multiplexed assay detection is a cross-sensitivity between the assays or due to signal cross-talk. Similar to a previously described investigation with a preliminary chip design,<sup>43</sup> the biosensing performance was rigorously tested for any cross-diffusion of hydrogen peroxide molecules between neighboring channels. As this can only happen during a stop-phase, the distance between neighboring immobilization sections was designed sufficiently. The cross-sensitivity measurements, shown in the Supporting Information, prove that even with stop-times up to 10 min, no cross-diffusion occurs.

**$\text{H}_2\text{O}_2$  Sensitivity.** Prior to the application of the platform with enzyme-linked assays providing a signal transduction via the formation of hydrogen peroxide, the  $\text{H}_2\text{O}_2$  sensitivity of the electrochemical cell is measured. For the calibration, the different chip formats are exposed to distinct concentrations of  $\text{H}_2\text{O}_2$ , prepared from a 30% (w/w) stock solution (Sigma-Aldrich), with an applied flow rate of 20  $\mu\text{L min}^{-1}$  per channel. Consequently, the  $\text{H}_2\text{O}_2$  sensitivity is determined to 2.14  $\mu\text{A cm}^{-2} \mu\text{M}^{-1}$  with an overall CV of <5% for different fabrication batches.

**Antibiotic Assay Calibration.** For the simultaneous detection of tetracycline and the streptogramin antibiotic pristinamycin in a clinically relevant sample, a calibration curve from each antibiotic is required. Thus, the assays for tetracycline and pristinamycin are first tested and characterized separately on-chip. Each assay step is prepared in 10 mM PBS (pH 7.4, 138 mM NaCl, 2.7 mM KCl) and optimized especially regarding the concentrations and incubation times of the assay components. For further details, the interested reader is referred to the Supporting Information. Upon finalizing the optimization of the assay parameters, calibration curves of each antibiotic are recorded. Therefore, different concentrations of a certain antibiotic are loaded to the different immobilization sections of an 8-channel chip via the individual inlets. Thus, 50  $\mu\text{g mL}^{-1}$  of the anti fluorescein antibodies are incubated for 1 h, and the channel surface is blocked for another hour with 1%

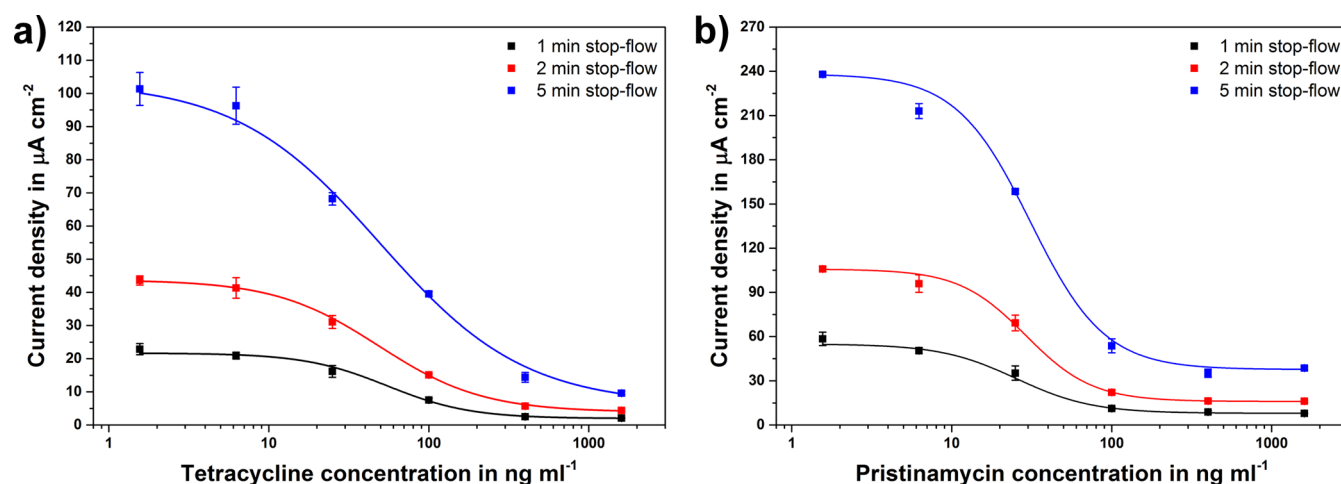


**Figure 4.** Calibration curves for tetracycline (a) and pristinamycin (b) in undiluted human plasma for different stop-flow times (1, 2, and 5 min). Increasing the stop-time enhances the assay signal. The results are fitted with a 4 parameter logistic curve gaining an interassay CV of <10% and LODs of 6.33 and 9.22  $\text{ng mL}^{-1}$  for tetracycline and pristinamycin, respectively.

(w/v) BSA in a 10 mM PBS solution. Subsequently, the individual sections are loaded for 15 min with either 0.1  $\mu\text{M}$  *tetO* or *Pir*.

The calibration measurements are executed in human plasma spiked with different antibiotic concentrations. Thus, they are mixed for 5 min with either 0.2  $\mu\text{g mL}^{-1}$  TetR or 2  $\mu\text{g mL}^{-1}$  PIP and 1  $\mu\text{g mL}^{-1}$  GOx. The respective solutions are subsequently incubated for 5 min in the immobilization sections. Between each assay step, the microfluidic network is temporarily sealed and flushed with 50  $\mu\text{L}$  per channel of wash buffer (10 mM PBS containing 0.05% Tween 20), introduced from the common outlet. The resulting curves for either 1, 2, or 5 min stop-flow are illustrated in Figure 4. As expected, the assay signal decreases with increasing antibiotic concentration for both antibiotics. This signal behavior is typical for competitive assays and can be fitted with a 4 parameter logistic (4PL) curve. The main parameters obtained from the fitted data are summarized in Table 1.

**Table 1.** Antibiotic Assay Parameters Obtained from the Fitted (4PL) Calibration Curves for 2 min Stop-Flow

	tetracycline	pristinamycin
IC50 in $\text{ng mL}^{-1}$	48.78	29.02
fit quality	0.9974	0.9990
slope	1.3352	2.0829
LOD in $\text{ng mL}^{-1}$	6.33	9.22
interassay precision (CV) in %	<10	<10
mean $I_0$ values (2 min) in $\mu\text{A cm}^{-2}$	43.74 $\pm$ 2.56	127.38 $\pm$ 5.82

The investigated concentration range shows a strong correlation to the fitted plot. All measured values do not exceed an interassay CV of 10%. Nevertheless, the overall signal of pristinamycin is higher than the one of tetracycline. This is due to the need for a higher concentration of bPIP required to achieve an optimal assay performance. This indicates a different sensitivity and reactivity of the two repressor proteins toward their respective antibiotics. For most of the screening applications with regard to these antibiotics, the LODs are more than sufficient. The concentrations for POC testing, according to the regulations by the EU, are in the range of hundreds of  $\text{ng mL}^{-1}$ . For tetracycline, for example, 100  $\text{ng mL}^{-1}$

is considered as a maximum residue level (MRL) in milk samples and up to 600  $\mu\text{g kg}^{-1}$  in meat specimens.<sup>44</sup>

**Simultaneous Measurement.** Once the optimization of the assay procedure and the determination of the calibration curves for both antibiotics are fulfilled, the simultaneous detection of tetracycline and pristinamycin from the same specimen is performed in spiked human plasma. As illustrated in Figure 5a, alternating immobilization sections of the 4-channel chips are prepared either with tetracycline or pristinamycin operator DNAs. Samples are spiked with 50  $\text{ng mL}^{-1}$  tetracycline and 10  $\text{ng mL}^{-1}$  pristinamycin. Additionally, the final sample solutions contain 1  $\mu\text{g mL}^{-1}$  avidin-GOx, 0.2  $\mu\text{g mL}^{-1}$  and 2  $\mu\text{g mL}^{-1}$  of bTetR and bPIP. The sample mix is then incubated in all channels for 5 min. In contrast to the POC scenario depicted in Figure 5b, the assay reagents for this measurement are also introduced by the individual inlets.

After removing the unbound proteins with wash buffer, glucose is introduced and the amperometric signals are read out with a 2 min stop-flow protocol. The reproducibility is examined by the measurement of three different 4-channel chips each comprising duplicates for both antibiotics ( $n = 3 \times 2$ ). The 2 min stop-flow signals collected by the simultaneous detection of 50  $\text{ng mL}^{-1}$  tetracycline and 10  $\text{ng mL}^{-1}$  pristinamycin, compared to their predicted values from the calibration curves are presented in Figure 5c. The measurements of the immobilization sections prepared for tetracycline reveal an average current density of  $25.2 \pm 2.67 \mu\text{A cm}^{-2}$ . From the calibration curve  $22.1 \mu\text{A cm}^{-2}$  are expected for 50  $\text{ng mL}^{-1}$  tetracycline resulting in a recovery of 113.9%. For the measurements of 10  $\text{ng mL}^{-1}$  pristinamycin an average current density of  $85.32 \pm 7.78 \mu\text{A cm}^{-2}$  is obtained. In comparison to the expected value of  $96.7 \mu\text{A cm}^{-2}$ , a recovery yield of 88% is achieved. The simultaneous quantification of 50  $\text{ng mL}^{-1}$  tetracycline and 10  $\text{ng mL}^{-1}$  pristinamycin in plasma samples is carried out with interassay CVs of 11% and 7%, respectively.

**Long-Term Storage.** For point-of-care testing the measurement scenario, as depicted in Figure 5b, represents the ideal case. Therefore, the storage conditions and the shelf life of the biosensors are crucial issues. In the case of on-site applications, the chips should be preimmobilized with the



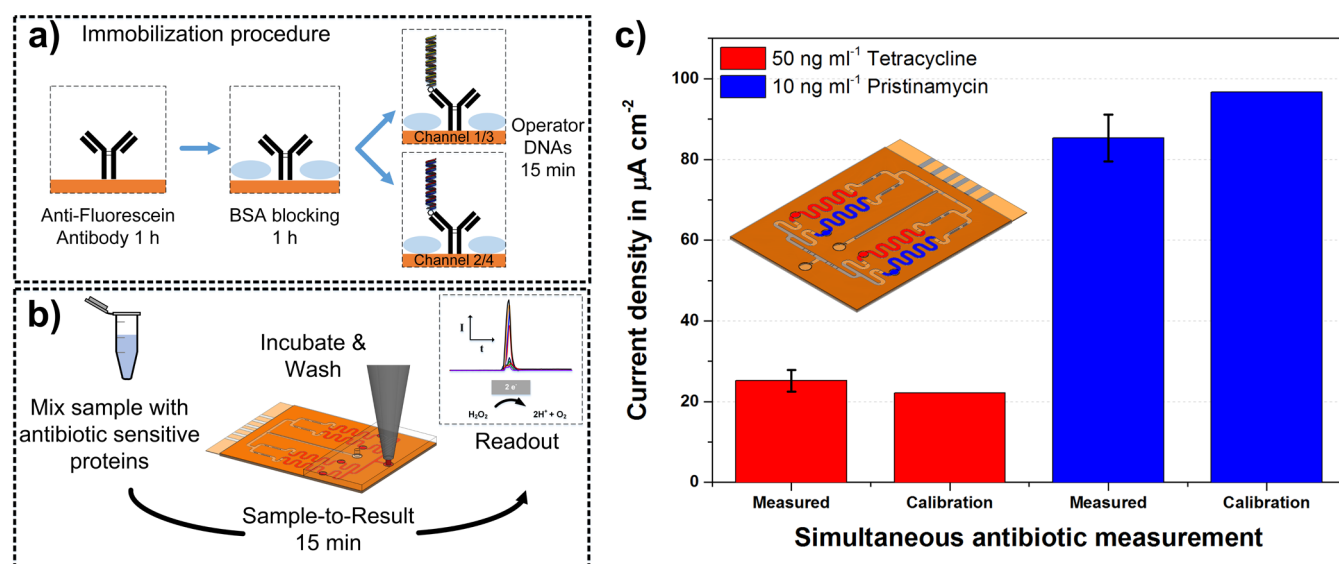


**Figure 5.** (a) Immobilization procedure of the DNA-based antibiotic assays. Different immobilization sections are prepared with the relevant operator DNAs. (b) POC measurement scenario for the quantification of antibiotics. The sample is mixed with the repressor proteins and incubated to the preimmobilized chips. After a washing step, the electrochemical signal readout is performed. (c) Data obtained from simultaneous measurements of the two antibiotics tetracycline and pristinamycin in spiked plasma. The signals are compared to the calculated values from the respective calibration curve. Thereby, three 4-channel chips are prepared with the assays for tetracycline and streptogramin in two channels each ( $n = 3 \times 2$ ), as illustrated in the inset.

antifluorescein antibodies, blocked with BSA and incubated with the desired DNA strand. An ideal sensor device provides a facile storage (e.g., at RT or +4 °C) facilitating an extended shelf life without losing its functionality.

In order to validate the storage conditions and shelf life of our platform, a 3-month survey of preimmobilized biosensor chips is performed in this work. Different biosensor chips are incubated with antifluorescein antibodies, blocked with BSA, and subsequently functionalized with the oligonucleotides *tetO*. Upon a 1 min drying, the microfluidic chips are sealed airtight together with a desiccant and stored in a refrigerator at 4 °C. For each test, the chips are incubated with the protein solution, containing bTetR and avidin-GOx, and measured by a 2 min stop-flow protocol. The results of the shelf life study of the biosensor chips using the tetracycline assay for a period of 3 months are illustrated in Figure 6. The results reveal that the biosensor chips can easily be stored for longer periods while maintaining their full functionality. The measured signals show an excellent reproducibility and precision after several months with a maximum intra-assay CV of 5.8% and an overall interassay CV of 13.1%. Pursuant to this long-term study is the surface of the employed dry film photoresist, Pyralux PC1025 offers the possibility for a stable and facile biomolecule storage.

## CONCLUSION

We present the development and the application of a low-cost microfluidic platform for the simultaneous electrochemical detection of multiplexed assays in clinically relevant samples. In this context, a compact and sensitive biosensor aiming for future point-of-care detection of different antibiotics was designed. The advantageous dry film photoresist technology is employed for the reproducible wafer-level fabrication of robust and flexible biosensor chips. The electrochemical and biochemical evaluation of the microfluidic multiplexed POC platform are successfully accomplished. Although different assays are immobilized in close proximity, no cross-sensitivity

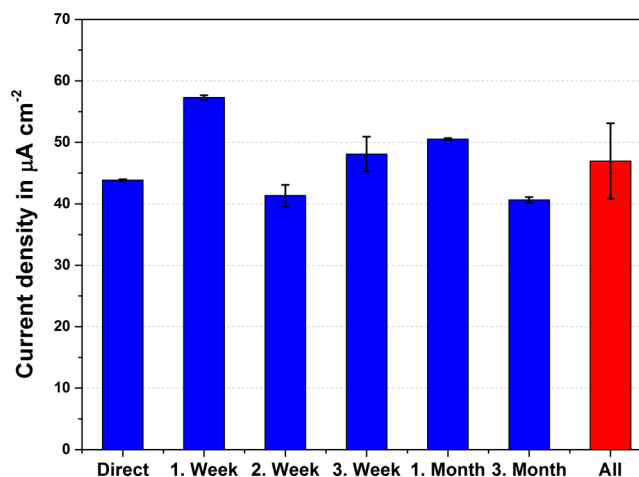


**Figure 6.** Results for a 3-month survey of preimmobilized biosensors using the tetracycline assay. For the measurement repressor proteins bound to GOx are added. The assay signals are measured with a 2 min stop-flow protocol in duplicates.

due to diffusion is observed. Enabled by a passive valving system and pressure driven flow, the on-chip detection of different enzyme-linked assays is realized.

Furthermore, the system is investigated for its applicability for multiplexed antibiotic detection via very sensitive and class-specific repressor/operator DNA-based assays. They are adapted and optimized for the immobilization in the microfluidic channel network and the electrochemical readout. A simultaneous detection of two antibiotics from spiked plasma samples is successfully shown. Detection limits of 6.33 and 9.22 ng mL<sup>-1</sup> are achieved for tetracycline and pristinamycin, respectively. With regard to a possible application in stock farmings and veterinary medicine, the investigated concentration range is sufficiently covered. In the future, this platform will be integrated to a hand-held reader including a micro pump



and a compact control unit. Especially the fast measurement along with preimmobilized chips brings the platform closer to a POC antibiotic screening application with sample-to-result times of less than 15 min. In summary, the progress toward disposable, easy-to-handle sensors for a wide range of ELA-based applications is brought further. This study reveals a universal and simple multianalyte sensor platform that combines the advantages of microfluidics, electrochemical biosensors and enzyme-linked assays.

## ■ ASSOCIATED CONTENT

### Supporting Information

The Supporting Information is available free of charge on the ACS Publications website at DOI: [10.1021/acs.analchem.6b02294](https://doi.org/10.1021/acs.analchem.6b02294).

Detailed illustration of the chip fabrication, measurement setup, H<sub>2</sub>O<sub>2</sub> sensitivity and cross-sensitivity tests, and antibiotic assay optimization (PDF)

## ■ AUTHOR INFORMATION

### Corresponding Author

\*E-mail: [dincer@imtek.de](mailto:dincer@imtek.de). Phone: +49 761 203 7264. Fax: +49 761 203 7262.

### Present Address

<sup>||</sup>L.A. and A.K.: ETH Zurich, Department of Biosystems Science and Engineering, Vladimir-Prelog-Weg 1-5/10, CH-8093 Zurich.

### Author Contributions

<sup>†</sup>A.K. and C.C. contributed equally to this work.

### Notes

The authors declare no competing financial interest.

## ■ ACKNOWLEDGMENTS

The authors would like to thank the German Research Foundation (DFG) for partially funding this work under Grant Numbers UR 70/10-01, WE 4733/4, and EXC-294 (BIOSS). Additionally, we thank the University Medical Center Freiburg, Germany, for providing human plasma samples.

## ■ REFERENCES

- (1) Gauglitz, G. *Annu. Rev. Anal. Chem.* **2014**, *7*, 297–315.
- (2) Choi, S.; Goryll, M.; Sin, L. Y. M.; Wong, P. K.; Chae, J. *Microfluid. Nanofluid.* **2011**, *10*, 231–247.
- (3) Wang, J. *Biosens. Bioelectron.* **2006**, *21*, 1887–1892.
- (4) Song, Y.; Huang, Y. Y.; Liu, X.; Zhang, X.; Ferrari, M.; Qin, L. *Trends Biotechnol.* **2014**, *32*, 132–139.
- (5) Chin, C. D.; Linder, V.; Sia, S. K. *Lab Chip* **2012**, *12*, 2118–2134.
- (6) Yager, P.; Edwards, T.; Fu, E.; Helton, K.; Nelson, K.; Tam, M. R.; Weigl, B. H. *Nature* **2006**, *442*, 412–418.
- (7) Kling, J. *Nat. Biotechnol.* **2006**, *24*, 891–893.
- (8) Rusling, J. F. *Anal. Chem.* **2013**, *85*, 5304–5310.
- (9) Nikaido, H. *Annu. Rev. Biochem.* **2009**, *78*, 119–146.
- (10) World Health Organization. Fact sheet No. 194, *Antimicrobial Resistance*, <http://www.who.int/mediacentre/factsheets/fs194/en/> (accessed February 24, 2016).
- (11) Cháfer-Pericás, C.; Maquieira, Á.; Puchades, R. *TrAC, Trends Anal. Chem.* **2010**, *29*, 1038–1049.
- (12) Kloth, K.; Rye-Johnsen, M.; Didier, A.; Dietrich, R.; Märklbauer, E.; Niessner, R.; Seidel, M. *Analyst* **2009**, *134*, 1433–1439.
- (13) Bradbury, A.; Pluckthun, A. *Nature* **2015**, *518*, 27–29.
- (14) Link, N.; Weber, W.; Fussenegger, M. *J. Biotechnol.* **2007**, *128*, 668–680.
- (15) Poole, K. *Ann. Med.* **2007**, *39*, 162–176.
- (16) Weber, C. C.; Link, N.; Fux, C.; Zisch, A. H.; Weber, W.; Fussenegger, M. *Biotechnol. Bioeng.* **2005**, *89*, 9–17.
- (17) Hacia, J. G. *Nat. Genet.* **1999**, *21*, 42–47.
- (18) Bernard, A.; Michel, B.; Delamarche, E. *Anal. Chem.* **2001**, *73*, 8–12.
- (19) Spindel, S.; Sapsford, K. E. *Sensors* **2014**, *14*, 22313–22341.
- (20) Wilson, M. S.; Nie, W. *Anal. Chem.* **2006**, *78*, 2507–2513.
- (21) Dunbar, S. A. *Clin. Chim. Acta* **2006**, *363*, 71–82.
- (22) Honda, N.; Lindberg, U.; Andersson, P.; Hoffmann, S.; Takei, H. *Clin. Chem.* **2005**, *51*, 1955–1961.
- (23) Ko, Y. J.; Maeng, J. H.; Ahn, Y.; Hwang, S. Y.; Cho, N. G.; Lee, S. H. *Electrophoresis* **2008**, *29*, 3466–3476.
- (24) Sato, K.; Yamanaka, M.; Takahashi, H.; Tokeshi, M.; Kimura, H.; Kitamori, T. *Electrophoresis* **2002**, *23*, 734–739.
- (25) Wang, J.; Liu, G.; Merkoçi, A. *J. Am. Chem. Soc.* **2003**, *125*, 3214–3215.
- (26) Ghodbane, M.; Stucky, E. C.; Maguire, T. J.; Schloss, R. S.; Shreiber, D. I.; Zahn, J. D.; Yarmush, M. L. *Lab Chip* **2015**, *15*, 3211–3221.
- (27) Dungchai, W.; Chailapakul, O.; Henry, C. S. *Anal. Chem.* **2009**, *81*, 5821–5826.
- (28) Taranova, N. A.; Berlina, A. N.; Zherdev, A. V.; Dzantiev, B. B. *Biosens. Bioelectron.* **2015**, *63*, 255–261.
- (29) Whitesides, G. M. *Nature* **2006**, *442*, 368–373.
- (30) Chin, C. D.; Laksanasopin, T.; Cheung, Y. K.; Steinmiller, D.; Linder, V.; Parsa, H.; Wang, J.; Moore, H.; Rouse, R.; Umvilighozo, G.; Karita, E.; Mwambarangwe, L.; Braunstein, S. L.; van de Wiggert, J.; Sahabo, R.; Justman, J. E.; El-Sadr, W.; Sia, S. K. *Nat. Med.* **2011**, *17*, 1015–1019.
- (31) Araz, M. K.; Tentori, A. M.; Herr, A. E. *J. Lab. Autom.* **2013**, *18*, 350–366.
- (32) Bange, A.; Halsall, H. B.; Heineman, W. R. *Biosens. Bioelectron.* **2005**, *20*, 2488–2503.
- (33) Kwakye, S.; Goral, V. N.; Baeumner, A. J. *Biosens. Bioelectron.* **2006**, *21*, 2217–2223.
- (34) Díaz-González, M.; Muñoz-Berbel, X.; Jiménez-Jorquera, C.; Baldi, A.; Fernández-Sánchez, C. *Electroanalysis* **2014**, *26*, 1154–1170.
- (35) Ghindilis, A. L.; Smith, M. W.; Schwarzkopf, K. R.; Roth, K. M.; Peyvan, K.; Munro, S. B.; Lodes, M. J.; Stöver, A. G.; Bernards, K.; Dill, K.; McShea, A. *Biosens. Bioelectron.* **2007**, *22*, 1853–1860.
- (36) Kadimisetty, K.; Malla, S.; Sardesai, N. P.; Joshi, A. A.; Faria, R. C.; Lee, N. H.; Rusling, J. F. *Anal. Chem.* **2015**, *87*, 4472–4478.
- (37) Piraino, F.; Volpetti, F.; Watson, C.; Maerkl, S. J. *ACS Nano* **2016**, *10*, 1699–1710.
- (38) Horak, J.; Dincer, C.; Bakirci, H.; Urban, G. *Biosens. Bioelectron.* **2014**, *58*, 186–192.
- (39) Armbrrecht, L.; Dincer, C.; Kling, A.; Horak, J.; Kieninger, J.; Urban, G. *Lab Chip* **2015**, *15*, 4314–4321.
- (40) Oh, K. W.; Lee, K.; Ahn, B.; Furlani, E. P. *Lab Chip* **2012**, *12*, 515–545.
- (41) Weltin, A.; Kieninger, J.; Enderle, B.; Gellner, A. K.; Fritsch, B.; Urban, G. A. *Biosens. Bioelectron.* **2014**, *61*, 192–199.
- (42) Menzel, A.; Gübeli, R. J.; Güder, F.; Weber, W.; Zacharias, M. *Lab Chip* **2013**, *13*, 4173–4179.
- (43) Kling, A.; Dincer, C.; Armbrrecht, L.; Horak, J.; Kieninger, J.; Urban, G. *Procedia Eng.* **2015**, *120*, 916–919.
- (44) The European Commission. *Off. J. Eur. Union* **2010**, *L15*, 1–72.